1 The importance of non-stationary multiannual periodicities in the NAO index for forecasting

2 water resource drought

3 William Rust [a]; John P Bloomfield [b]; Mark Cuthbert [cd]; Ron Corstanje [e]; Ian Holman [a]

4 a Cranfield Water Science Institute (CWSI), Cranfield University, Bedford MK43 0AL
5 b British Geological Survey, Wallingford, OX10 8BB
6 c School of Earth and Environmental Sciences, Cardiff University, Park Place, Cardiff, CF10
7 3AT
8 d School of Civil and Environmental Engineering, The University of New South Wales,
9 Sydney, Australia
10 e Centre for Environment and Agricultural Informatics, Cranfield University, Bedford MK43
11 0AL
12
13 Correspondence to Ian Holman (i.holman@cranfield.ac.uk)

14 **Abstract**

15 Drought forecasting and early warning systems for water resource extremes are increasingly

16 important tools in water resource management in Europe where increased population

17 density and climate change are expected to place greater pressures on water supply. In this

18 context, the North Atlantic Oscillation (NAO) is often used to indicate future water resource

19 behaviours (including droughts) over Europe, given its dominant control on winter rainfall

20 totals in the North Atlantic region. Recent hydroclimate research has focused on the role of

21 multiannual periodicities in the NAO in driving low frequency behaviours in some water

22 resources, suggesting that notable improvements to lead-times in forecasting may be

23 possible by incorporating these multiannual relationships. However, the importance of

24 multiannual NAO periodicities for driving water resource behaviour, and the feasibility of this

25 relationship for indicating future droughts, has yet to be assessed in the context of known

26 non-stationarities that are internal to the NAO and its influence on European meteorological

27 processes. Here we quantify the time-frequency relationship between the NAO and a large

28 dataset of water resources records to identify key non-stationarities that have dominated

29 multiannual behaviour of water resource extremes over recent decades. The most dominant

30 of these is a 7.5-year periodicity in water resource extremes since approximately 1970 but

31 which has been diminishing since 2005. Furthermore, we show that the non-stationary

relationship between the NAO and European rainfall is clearly expressed at multiannual

periodicities in the water resource records assessed. These multiannual behaviours are

found to have modulated historical water resource anomalies to an extent that is comparable

to the projected effects of a worst-case climate change scenario. Furthermore, there is

limited systematic understanding in existing atmospheric research for non-stationaries in

these periodic behaviours which poses considerable implications to existing water resource

forecasting and projection systems, as well as the use of these periodic behaviours as an

indicator of future water resource drought.

1. Introduction

Oscillatory ocean-atmosphere systems (such as El Nino Southern Oscillation (ENSO), North

Atlantic Oscillation (NAO) and Pacific Decadal Oscillation (PDO)) are known to modulate

hydrometeorological processes over a large domain, often driving multiannual periodicities in

hydrological records (Kuss and Gurdak, 2014; Labat, 2010; Trigo et al., 2002). As such,

indices of these systems can be useful when explaining decadal-scale variations in water

resource behaviour in Europe (Svensson et al, 2015; Kingston et al, 2006), North America

(Coleman and Budikova, 2013) and Asia (Gao et al, 2021). In the North Atlantic region, the

NAO represents the principal mode of atmospheric variability and is a leading control on

European winter rainfall totals (Hurrel, 1995; Hurrel and Deser, 2010). As such, many

studies have found strong and significant relationships between the winter NAO Index

(NAOI) and hydrological variables across Europe (Wrzesinski and Paluszkiewicz, 2011;

Brady et al, 2019; Burt and Howden, 2013), leading to the development of seasonal and

long-lead forecasting systems of hydrological behaviour (Svensson et al, 2015, Bonaccorso

et al, 2015).

A growing number of studies have identified stronger relationships between the NAOI and

certain water resource variables at multiannual periodicities (Holman et al, 2011; Neves et

al, 2019; Uvo et al, 2021), than at an annual scale. This is particularly apparent where longer

hydrological response times predominate (Rust et al 2021a). For instance, Neves et al

(2019) identified significant relationships between the NAOI and groundwater level in

Portuguese aquifers and at approximately 6- and 10-year periodicities, with associations to

episodes of recorded groundwater drought. Furthermore, Liesch and Wunsch (2019) found

significant coherence between NAOI and groundwater level at approximately 6- to 16-year

periodicities across the UK, Germany, Netherlands and Denmark. Rust et al (2019; 2021a)

identified a similar significant 6- to 9-year cycle across a large dataset of groundwater level

(59 boreholes) and streamflow (705 gauges) in the UK, which was associated with the

principal periodicity of the NAO (of a similar length (Hurrell et al., 2003; Zhang et al., 2011)).

In the instance of groundwater level, this periodicity was found to represent a notable portion

of overall behaviour (40% the standard deviation), and minima in the cycle were shown to

align with recorded instances of wide-spread groundwater drought (Rust et al, 2019). Given

their association with recorded droughts across Europe, these studies highlight the potential

benefit of an *a priori* knowledge of multiannual NAO periodicities in water resources for

improving preparedness for water resource drought in Europe. While water resources may

refer to multiple types of hydrological stores (e.g., streamflow, groundwater, reservoirs and

lakes), in this paper we are exclusively considering streamflow and groundwater stores.

However, the value of a multiannual relationship between the NAO and European water

resources has yet to be assessed in the context of reported non-stationarities in

hydroclimate systems. For instance, the NAO is an intrinsic mode of atmospheric variability

(Deser et al, 2017), but can also be influenced by multiple other teleconnection systems

such as the Madden-Julien Oscillation, Quasi-Biennial Oscillation (Feng et al 2021) or El-

Nino Southern Oscillation (Zhang et al, 2019). As such it is currently unclear whether

periodicities in the NAOI are emergent behaviours or the result of external forcing. This has

been compounded by a relatively weak signal-to-noise ratio for NAO periodicities, making

confident multiannual signal detection difficult (O'Reilly et al, 2018; Hurrel et al, 1997).

85   Stronger NAO-like multiannual periodicities have been detected in water resource variables

86   in both wet and dry seasons (Rust et al, 2021b), even where weaker relationships exist

87   between winter NAOI and summer water resources (e.g., West et al (2022)), due to the

88   high-band filtering function and protracted response of some hydrological processes (van

89   Loon, 2013).However, the degree to which these behaviours are sufficiently stable to enable

90   development of predictive utilities is currently unclear. Furthermore, existing research has

91   shown that the sign of the relationship between NAOI and European rainfall is non-stationary

92   at decadal timescales (Rust et al, (2021b); Vicente-Serrano and López-Moreno (2008)). This

93   is expected to add a degree of uncertainty to the detection of lead times between

94   multiannual periodic components in the NAO and water resource response, which is

95   necessary in the development of early warning systems for water resource drought. While

96   some studies have ascribed lags to this multiannual relationship for European water

97   resources (Neves et al, 2019; Holman et al, 2011), the extent to which this non-stationarity is

98   present at multiannual periodicities has yet to be assessed.

99   Finally, a critical application of early warning systems for water resource extremes is in the

100   design of drought management regimes for existing and projected climate change (Sutanto

101   et al, 2020). While some studies have quantified the degree of modulation that multiannual

102   ocean-atmosphere systems can have on water resources (Kuss and Gurdak, 2014; Neves et

103   al., 2019; Velasco et al., 2015), few have compared these to the expected modulations from

104   projected climate change scenarios. As such the benefit of incorporating multiannual NAO

105   periodicities into early warning systems for improving preparedness for water resource

106   extremes in climate change scenarios has not been assessed.

107   The aim of this paper is to assess the utility of multiannual relationships between the NAO

108   and water resources for improving preparedness for future water resource drought. This aim

109   will be met by addressing the following research objectives:

1. Quantify significant covariances between multiannual periodicities in the NAOI and water resource extremes, and assess the extent to which these periodicities are stable over time

2. Assess multiannual periodicity phase differences between the NAOI and water resources over time, to understand the extent to which annual-scale non-stationarities between the NAO and rainfall in the UK are expressed at multiannual scales

3. Quantify the modulations of water resource variables caused by key multiannual periodicities in the NAO, during the dry season, and compare this with projected modulations of water resources due to climate change.

These objectives will be implemented on UK water resource records, given the considerable coverage of recorded water resource data in time and across the space (Marsh and Hannaford, 2008); however, the implications of findings for the UK will be discussed within a wider European context.

2. Data

2.1.   Water resource data

The National Groundwater Level Archive (NGLA) and National River Flow Archive (NRFA) provide high-resolution spatiotemporal coverage of groundwater level records and streamflow across the UK.

2.1.1. Groundwater data

Monthly NGLA groundwater level data from 136 boreholes covering all of the major UK aquifers, with record lengths of more than 20 years and data gaps no longer than 24 months, have been used (Figure 1). While some meta-analysis was conducted on monthly data, the primary analysis was undertaken on seasonally averaged data, meaning a data gap of no more than two points. They cover a range of unconfined and confined consolidated aquifer

types and have been categorised into generalised aquifer groups of Chalk (78 sites), Limestone (12 sites), Oolite (12 sites), Sandstone (34) and variably cemented mixed clays and sands (Lower Greensand Group, Allen et al., 1997) (3 sites). Given the spatially heterogenous response of the Chalk aquifer to droughts (Marchant and Bloomfield, 2018), Chalk sites have been subdivided into four groups based on aquifer region: Lincolnshire basin (8 sites), East Anglian basin (17 sites), Thames and Chiltern basin (29 sites) and Southern basin (21 sites) (Allen et al., 1997; Marchant and Bloomfield, 2018).

Broad aquifer groups can be described as follows: Chalk, a limestone aquifer comprising of a dual porosity system with localized areas where it exhibits confined characteristics; characterised by fast-responding fracture porosity (Bloomfield, 1996); Oolite characterised by a highly fractured lithology with low intergranular permeability; Sandstone, comprised of sands silts and muds with principle inter-granular flow but fracture flow where fractures persist; and Lower Greensand, characterised by intergranular flow with lateral fracture flow depending on depth and formation (Allen et al, 1997).

2.1.2. Streamflow data

Monthly streamflow data from the UK National River Flow Archive (NRFA; Dixon et al., 2013: http://nrfa.ceh.ac.uk/) has been used. Gauging stations with more than 20 years of continuous streamflow data and no data gaps greater than 24 months were initially selected. Sites serving the largest catchment were selected where there are multiple sites within a single river catchment. This produced a final list of 767 streamflow gauging stations for use. To understand broad spatial relationships across the streamflow dataset, records have been divided into groups based on the NRFA river drainage basin (RDB). These are grouped by seven generalised regions of the UK; North and West Scotland (75 records), East Scotland (89 records), Northern Ireland (38 records), North-west England (70 records), North-east England (102 records), Wales & South-west England (170 records), East Anglia & South-east England (223 records). Streamflow with minimal influence from human factors is often used in hydroclimate studies to avoid confounding mechanisms, however no such large-scale

163   dataset exists for the UK. Furthermore, over the period of analysis and the broad scale of this

164   assessment, inconsistences in the way water resource management practices are

165   implemented is expected to result in noise to the observations rather than some systematic

166   signal or bias that would affect the results of this paper.

167   2.2.   North Atlantic Oscillation data

168   Monthly North Atlantic Oscillation Index (NAOI) data calculated by the National Centre for

169   Atmospheric Research (NCAR) using the principal component (PC) method for the period

170   1899 – 2021 has been used. The PC NAOI is a time series of the leading empirical orthogonal

171   functions (EOFS) of sea level pressure grids across the north Atlantic region (20°-80°N, 90°W-

172   40°E).

173
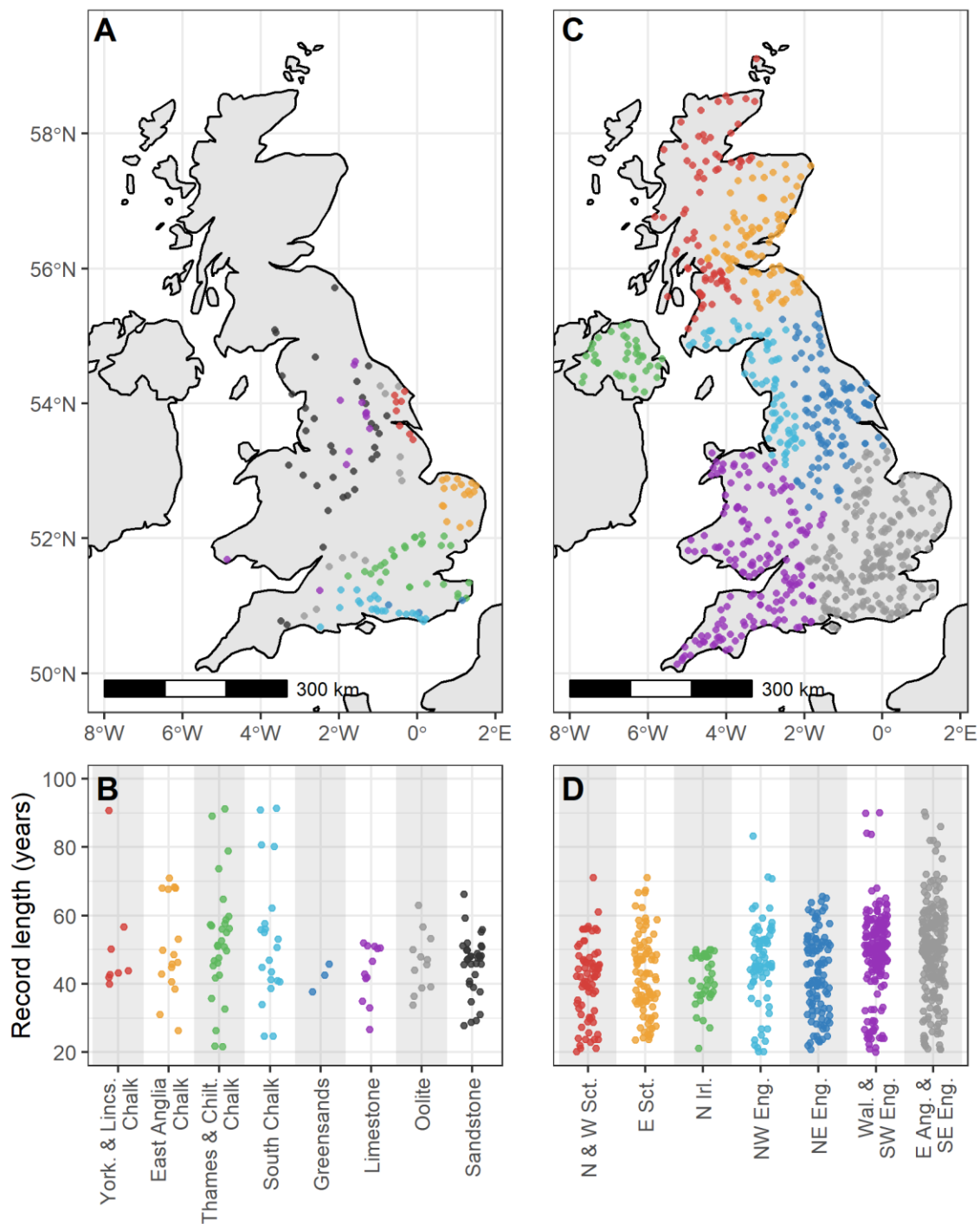
Figure 1 – Spatial and temporal distributions of water resource records; a) location of groundwater boreholes coloured by associated aquifer group, b) jitter plot of groundwater record lengths within each aquifer group, c) location of streamflow gauges coloured by associated regional group, d) jitter plot of streamflow record lengths within each regional group

178

179

3. Methods

3.1. Data Pre-processing

In this study we use the continuous and cross-wavelet transform to understand behaviours and relationships across different periodicities within the different water resource variable time series.

Only records with a data length of 20 years or greater have been used in this analysis to ensure that all of the sites have sufficient data to quantify (as a minimum) the strength of the dominant ~7-year cycle detected in water resources in previous research. Here, we assess periodicities between 2 and 32 years. The wavelet transform provides an instantaneous measure of frequency power within a dataset, as such it can quantify periodicities beyond the length of the dataset but with lower precision. The median record length of groundwater is 48years, and 47 years in streamflow, meaning the influence of these records on the detection of periodicities up to 32 years is expected to be minimal.

For all datasets, gaps less than two years were infilled to a monthly time step using a cubic spline to produce a complete time series for the wavelet transform. For time series with gaps greater than two years, the shortest time period before or after the data gap was removed. The records were not trimmed to obtain a common period of data coverage. Instead, all data was trimmed to start at a minimum of 1930. This was to allow the analysis of the fewer records that cover a longer time period while still capturing a time periods with adequate record coverage. All of the time series were standardised by dividing by their standard deviation and subtracting their mean.

Finally, three time-aggregated series for each water resource record have been used; monthly, winter-average (DJF) and summer average (JJA).

3.2. Quantifying wide-spread water resource drought

In order to meet objective 1, we produced a time series which describes the behaviour of wide-spread water resource drought across each resource variable (i.e., groundwater or

206   streamflow). In this study we use the drought threshold methodology proposed in Peters

207   (2003). While other measures of drought are available (e.g., Standardised Precipitation

208   Index (SPI) and Standardised Groundwater Index (SGI)) (Bloomfield and Marchant, 2013), a

209   threshold approach has been adopted as its can be easily applied to both streamflow and

210   groundwater variables.

211   To calculate a drought series from monthly groundwater level and streamflow series, we first

212   used the threshold methodology given by equation 5 from Peters (2003):

213

$$\int_0^M (x_t(c) - x(t))_+ \, dt = c \int_0^M (\bar{x} - x(t))_+ \, dt \qquad \text{(Eq. 5)}$$

214   Where:

215    $$x_+ = \begin{cases} x & if \ x \geq 0 \\ 0 & if \ x < 0 \end{cases}$$

216   and M is the full length of the data series. Here we use a threshold level of c = 0.3 for

217   groundwater level and c = 0.01 for streamflow. Peters et al (2003) found that a value of 0.3

218   for groundwater level was comparable to other commonly used thresholds. A value of 0.01

219   for streamflow was chosen as it produced a similar distribution of drought events as the

220   groundwater drought series. The chosen value of c for either variable is not expected to

221   affect the outcomes of the study as the focus is on the frequency structure of water resource

222   drought, rather than magnitude.

223   For each measurement site, the monthly time series of drought status (whether in drought

224   according to the threshold criteria or not) was converted into a yearly series describing

225   whether that site experienced a drought in the calendar year. Then, for each year, the

226   number of sites that experienced drought were summed and divided by the number of sites

227   with coverage of that year. This produced a time series of the proportion of sites

228   experiencing drought each year, for groundwater level and streamflow variables. This is

229   referred to as the drought coverage time series. In the case of streamflow, this drought

230   series is analogous to low flows, however, when used in conjunction with a frequency

231   analysis of multi-year periodicities, the method assesses multi-year low flow conditions

232   which may be defined as drought.

3.3.   Frequency Transformations

3.3.1. Continuous Wavelet Transform (CWT)

235   The Continuous Wavelet Transform (CWT) was performed on the drought coverage time

236   series for groundwater and streamflow to understand the frequency behaviour of wide-

237   spread water resource drought over time. The CWT is often used in geoscience to

238   understand non-stationarities of a variable over time and frequency space (Sang, 2013).

239   The cross-wavelet transform, W, consists of the convolution of the data sequence (x_t) with

240   scaled and shifted versions of a mother wavelet (daughter wavelets):

$$W(\tau, s) = \sum_t x_t \frac{1}{\sqrt{s}} \psi * \left(\frac{t - \tau}{s} \right) \qquad \text{(Eq. 6)}$$

241   where the asterisk represents the complex conjugate, τ is the localized time index, s is the

242   daughter wavelet scale and dt is increment of time shifting of the daughter wavelet. The

243   choice of the set of scales s determines the wavelet coverage of the series in its frequency

244   domain. The Morlet wavelet was favoured over other candidates due to its good definition in

245   the frequency domain and its similarity with the signal pattern of the environmental time

246   series used (Tremblay et al. 2011; Holman et al. 2011).

247   The modulus of the transform can be interpreted as the continuous wavelet power (CWP):

$$P(\tau, s) = |W(\tau, s)| \qquad \text{(Eq. 7)}$$

248   The CWP is therefore an absolute measure of instantaneous frequency strength. We use the

249   package "WaveletComp" produced by Rosch & Schmidbauer (2018) for all wavelet

250   transformations in this paper.

251 The CWT was also undertaken on the summer-average water resource records for the

252 purpose of reconstructing the influence of dominant periodicities on dry-season water

253 resource behaviour.

254 3.3.2. Cross-Wavelet Transform (XWT)

255 The bivariate XWT was applied between the NAOI and each of the winter-average water

256 resources records (groundwater level (GWL) and streamflow (SF)). This produces a cross-

257 wavelet power which is analogous to the covariance between the two variables over a time

258 and frequency spectrum. This has been selected over the cross-wavelet coherence

259 (analogous to correlation) as this metric requires a high degree of spectral smoothing,

260 making the resultant coherence spectra sensitive to the choice of smoothing approach

261 (Rosch & Schmidbauer (2018)). Here we use the covariance spectrum to compare against

262 the drought series frequency spectrum to understand where strong coherences are reflective

263 of dominant behaviours in water resource drought.

264 In order to calculate cross-wavelet power (XWP) for the bivariate case, it is first necessary to

265 calculate the continuous wavelet transform (CWT) for each of the variables separately. The

266 XWT between variables x and y is given by:

$$W.xy(\tau,s) = \frac{1}{s} \cdot W.x(\tau,s) \cdot W.y*(\tau,s) \qquad \text{(Eq. 8)}$$

267 The modulus of the transform can be interpreted as the cross-wavelet power (XWP):

$$P.xy(\tau,s) = |W.xy(\tau,s)| \qquad \text{(Eq. 9)}$$

268

269 3.3.3. Wavelet Significance

270 Lag-1 autocorrelations (AR1) in environmental datasets can produce emergent low frequency

271 behaviours, making the detection of externally-forced behaviours more difficult (Allen and

272 Smith, 1996; Meinke et al., 2005; Velasco et al., 2015). In this study, a significance test was

273 undertaken to test the red-noise null hypothesis that wavelet powers calculated are the result

274   of the recorded variables' AR1 properties. This was based on 1000 synthetic Monte Carlo

275   series with the original AR1 values. In this paper we test significance to the 95% CI.

276   The significance spectra for the XWT for each variable pair (e.g., GWL and NAOI) form the

277   primary results for the XWT method in this paper, since the cross-wavelet power is heavily

278   dependent on the individual series and its frequency composition. The overall relationship

279   between the NAOI and water resources as a whole are investigated by showing the proportion

280   of sites over time and frequency that exhibit a significant relationship with the NAOI (95% CI).

281   This average significance spectrum is produced by summing the significance matrices across

282   each resource (groundwater level or streamflow) and dividing by the number of records used

283   in year each.

284

285   **3.3.4. Phase Difference**

286   In the bivariate case, the instantaneous phase difference for the XWP spectrum (between

287   wavelets pairs from the CWT spectrum for each variable) can also be calculated as:

$$Angle(\tau, s) = Arg(W.xy(\tau, s)) \hspace{3cm} \text{(Eq. 10)}$$

288

289   This is the difference of the individual phases from both variables at an instantaneous time

290   and frequency (period), converted to an angle between −π, and π. Values close to 0 indicate

291   the two series move in-phase, with absolute values close to π indicating an out-of-phase

292   relationship. Values between 0 and π indicate degrees of phase difference or phase shift.

293   Phase differences between 0 and π can indicate the degree to which variable x is leading

294   variable y, however a phase difference between 0 and -π can either indicate that variable y is

295   leading variable x, or that variable x is leading by more than half the phase rotation (period

296   length). The degree to which a certain variable is leading is analogous to a lag between the

297   two variables.

298

3.4.   Modulation measurement

In order to understand the degree of modulation that the NAO teleconnection has on water

resources, an absolute and relative modulation value has been calculated for each series.

Here, we use modulation to describe the degree to which the NAO (or other process) has

increased or decreased a water resource measure from its mean. This has been derived by

reconstructing a specific principal periodicity range from the cross-wavelet powers, within the

summer-average wavelet transform, using the following equation:

$$(x_t) = \frac{dj \cdot dt^{1/2}}{0.776 \cdot \psi(0)} \sum_s \frac{Re(W(.,s))}{s^{1/2}} \qquad \text{(Eq. 11)}$$

Where dj is the frequency step and dt is the time step.

This produces a periodic reconstruction of a component of the original dataset that conforms

to the set of periodicities (scale steps) selected within the summer-averaged water resource

records. The mean and maximum amplitude of this periodic reconstruction was calculated

from the absolute values of minima and maxima. Since the data were standardised by

dividing by the standard deviation prior to the wavelet transform, this calculated mean and

maximum amplitude are also relative to the sd of the original data. Multiplying the calculated

amplitude by the original sd converts this back into a real-valued measurement. This was

only done for groundwater, since streamflow is highly dependent on catchment size. In the

case of streamflow, amplitudes are reported as relative to the standard deviation of the

streamflow record. All calculated modulations were produced using reconstructed wavelets

from after 1970 where the majority of records are present in both groundwater and

streamflow variables. This was done to mitigate the effect of differing record lengths.

319

4. Results

4.1.   Multiannual water resource covariance with NAOI

322   Figure 2 shows the NAOI covariance significance spectrum (fig 2a and 2b) and drought

323   frequency spectrum (fig 2c and 2d) for the groundwater level records. These have been

324   plotted together to allow for easier interpretation and comparison of the results, and to

325   indicate broad-scale behaviours. Black lines in the spectral plots show the 95% CI. The

326   calculated drought series (fig 2e) and record coverage (fig 2f) have also been plotted

327   alongside for comparison.

328   Figure 2a shows the results from the XWT significance testing between the NAOI and the

329   136 groundwater level records. Results are displayed as contours showing the percentages

330   of sites that exhibited a significant (0.05 a) XWP within the time-frequency spectrum. There

331   are five localised regions within the NAOI x GWL XWP spectrum that denote a wide-spread

332   significance between the GWL records and the NAOI. The greatest significance contours of

333   these regions (referred to here as focal points (FPs)) are labelled on figure 2a as: FP 1: 1934

334   at the 4.2 years periodicity (80% of records); FP 2: 1974 at the 8.5 years periodicity (40% of

335   records); FP 3: 1995 at 5.4 years (80% of records); FP 4: 2005 at 7 years (90% of records)

336   and; FP 5: 2012 at 2.9 years (60% of records).

337   These focal points are grouped into three larger regions within the 10% contour; between

338   1933 – 1940 spanning the 3- to 5-year periodicity; 1964 – 2020 spanning the 4- to 12-year

339   periodicity and; 2007 – 2017 spanning the 2- to 4-year periodicity. There is a single peak in

340   the time-averaged percentage plots (figure 2b) at the 7.5-year periodicity (average of 26% of

341   records)

342   Figure 2c shows the results from the CWT of the groundwater drought series (shown in Fig

343   2e). There are five regions of significant wavelet power in the groundwater drought

344   frequency spectrum that are labelled in figure 2c as follows; region 1: 1930 - 1950 in the 4-

345   to 8-year periodicity range (greatest power at 4.8 years); region 2: 1930 – 1945 in the 10- to

346   13-year periodicity range (greatest power at 11.7 years); region 3: 1960 – 1965 in the 2.5- to

347   3.5-year periodicity range (greatest power at 2.8 years); region 4: 1960 – 1990 centred at the

348   12- to 17-year periodicity range (greatest power at 15.4 years); and region 5: 1980 to 2020

349   at the 6- to 8-year periodicity range (greatest power at 7 years). There is a sixth significant

350   region starting in 2019 and covering periods between 2 and 5 years, however this is very

351   close to the end of the record and may be subject to edge effects. As such this region has

352   not been taken forward for discussion.

353   There are also two notable non-significant regions of medium strength wavelet power (>=

354   0.4); 1930 - 2000 at the 14- to 23-year periodicity range (centred at 16 years), and between

355   1960 and 1970 at the 8- to 16-year periodicity range (centred at 9 years). There are two

356   notable peaks in time-averaged wavelet power for the GWL drought series (figure 2d); the

357   greatest at the 7-year periodicity (average wavelet power of 0.38), and the second at the 14-

358   year periodicity (average wavelet power of 0.24).

359   Figure 3 shows the same as Figure 2 but for the streamflow (SF) case. There are six

360   localised regions within the NAOI x SF XWP spectrum that denote a wide-spread

361   significance between the SF records and the NAOI. FPs of these regions are labelled on

362   figure 2a; FP 1: 1940 at the 6.7-year periodicity (30% of records); FP 2: 1962 at the 5.2-year

363   periodicity (50% of records); FP 3: 1975 at the 8.5-year periodicity (40% of records); FP 4:

364   1994 at the 5.2-year periodicity (80% of records); FP 5: 2007 at the 7-year periodicity (90%

365   of records) and; FP 6: 2011 to 2015 at the 3.2-year periodicity (60% of records). These

366   centres are grouped into larger regions within the 10% contour; these are between 1933 –

367   1947 spanning the 5.5- to 8-year periodicity; 1960 – 1970 spanning the 4- to 8-year

368   periodicity; 1965 – 1990 spanning the 7- to 11-year periodicity; 1988 – 2000 spanning the 4-

369   to 5.5-year periodicity; 1995 – 2020 spanning the 4.5- to 11-year periodicity and 2007 –

370   2017 spanning the 2.5- to 4.5-year periodicity. There is a single peak in the time-averaged

371   percentage plots (figure 3b) at the 7.5-year periodicity (average of 29% of records)

372   Figure 3c shows the results from the CWT of the streamflow drought series (shown in Fig

373   3e). There are three regions of significant wavelet power in the groundwater drought

374   frequency spectrum that are labelled on Figure 3c; region 1: 1930 – 1935 in the 21 year

375   periodicity (this region appears clipped by the record start date, so the strongest wavelet

376   power for this region may not be captured); region 2: 1930 - 1937 in the 2.5- to 6.5-year

377   periodicity range (strongest power at 4.3 years) and; region 3: 1930 – 1960 in the 11- to 15-

378   year periodicity range (strongest power at 13 years);

379   There are four non-significant regions of medium strength wavelet power (>= 0.4); 1935 –

380   1945 at the 2- to 3-year periodicity; 1955 – 1965 at the 2- to 4-year periodicity; 1960 – 2015

381   at the 5.5- to 8-year periodicity; and 2000 – 2005 at the 2- to 5-year periodicity. The time-

382   averaged wavelet power for the SF drought series (figure 3d) contains multiple peaks

383   suggesting no dominant periodicity. The greatest peak is at the 7-year periodicity with an

384   average wavelet power of 0.21.

385   **4.2.   Cross-wavelet phase difference**

386   The cross-wavelet phase difference (ϕ) between water resource variables and the NAOI at

387   the 7.5-year periodicity (identified as prevailing in the previous section) has been displayed

388   in figure 4 for the GWL records and figure 5 for the streamflow records. The phase difference

389   is a circular measurement where 0 indicates an in-phase relationship (analogous to zero lag)

390   and +/- π indicates an out-of-phase relationship between the selected periodicity within the

391   two variables (analogous to half a periodicity lag (3.75-years)). The purpose of these plots of

392   phase differences are to visualise and understand the difference in phase between the NAO

393   and water resources. Records have been split by their aquifer group in Figure 4, and by

394   catchment region in figure 5, to understand if there are any general differences between

395   regions.

396   The majority of groundwater level records cover the period 1970 to present, meaning

397   general trends are more clearly presented for this time period. The phase difference of most

398   GWL records can be defined by a sudden shift at approximately 1990 (figure 4). Values of ϕ

399   generally range from between -1/4π and -3/4π (-0.76 to -2.36 rads; generally anti-phase) for

400   the period 1975 to 1990 to between +1/4π and +3/4π (0.76 to 2.36 rads; generally in-phase)

401   for the period 1990 to 2019 across all sites. This is with the exception of 17 sites across the

402   South Chalk and Thames & Chiltern Chalk which have shorter ~anti-phase periods (between

403   approximately 1985 and 1990). Average φ values for the period 1970 – 1990 (1990 – 2020)

404   for each aquifer region are: -1.26 (1.41) in East Anglian Chalk; -2.25 (1.21) in Lincolnshire

405   Chalk, 0.52 (0.83) in South Chalk, -1.37 (0.83) in Thames & Chiltern Chalk, 1.51 (1.21) in

406   Greensands, -0.78 (0.66) in Limestone, -1.36 (1.09) in Oolite, -0.70 (1.35) in Sandstone. As

407   such most aquifer regions experience an average reversal of polarity at 1990. Greensand

408   GWL show no reversal when assessing average φ values, however 1 of the 3 sites in this

409   aquifer group does show this reversal.

410   Similar to the GWL records, most SF records exhibit a shift in phase difference at

411   approximately 1990, with catchment groups in the north of the UK showing minimal shifts

412   (i.e., NW Scotland, E Scotland, NI, and NW England) (figure 5). In the southern catchment

413   groups, values of φ generally range from between -1/2π and ±π (generally anti-phase) for

414   the period 1970-1990 (approximately prior to the shift) to between 0 and +3/4π (generally in-

415   phase) for the period 1990 to 2020 (approximately after the shift). Furthermore, catchment

416   groups in the east of the UK (i.e., E Scotland, NE England, East Anglia & SE England)

417   during the in-phase period (1990-2020) exhibit a notable transition to increased phase

418   difference (to approximately +3/4π) between 2000 and 2010 before decreasing to

419   approximately +1/4π in 2020. Average φ values for the period 1970 – 1990 (1990 – 2020)

420   for each catchment region are: -0.21 (0.14) in North and West Scotland, 0.49 (0.86) in East

421   Scotland, -0.43 (0.46) in Northern Ireland, -0.44 (0.47) in NW England, 2.32 (1.08) in NE

422   England, 0.77 (0.64) in Wales and SE England, and 2.53 (0.99) in East Anglia and SE

423   England.

424   4.3.   Modulation of dry season water resources

425   Figure 6 shows two boxplots for each aquifer group, representing the distribution of mean (in

426   blue) and maximum (in red) dry-season GWL deviation as a result of the 7.5-year periodicity

427   (over the length of each of the record). Median values from each of these mean and

428 maximum boxplots are described below, and are referred to as med.mean and med.max

429 respectively.

430 The 7.5 year periodicity accounts for the greatest deviation of-dry season GWL in the Chalk

431 aquifer regions, with the Thames & Chiltern basin GWL showing the greatest modulation of

432 all groups showing med.mean of 0.94m and a med.max of 1.38m. Two other Chalk groups

433 showed similarly strong modulations; the South Chalk basin GWL (med.mean: 0.7m,

434 med.max: 1.07m); and the Lincolnshire Chalk GWL (med.mean:.56m, med.max: 0.77m).

435 The East Anglia GWL show lowest modulation of the Chalk (med.mean: 0.16m, med.max:

436 0.34m), similar to GWL in the Limestone (med.mean: 0.35m, med.max: 0.51m) and the

437 Oolite (med.mean: 0.21m, med.max: 0.33m). Lowest overall modulations are found in the

438 Sandstone (med.mean: 0.15m, med.max: 0.25m) and Greensands aquifers (med.mean:

439 0.12m, med.max: 0.17m).

440 Figure 7 shows the same as figure 6 but for the streamflow case. Streamflow modulations

441 are measured as relative to the standard deviation of each record. Modulation of streamflow

442 for each catchment group are (in descending order of med.mean); Wales & south-west

443 England (med.mean: 0.32, med.max: 0.50); East Anglia & south-east England (med.mean:

444 0.31, med.max: 0.53); Northern Ireland (med.mean: 0.29, med.max: 0.50); West Scotland

445 (med.mean: 0.27, med.max: 0.46); north-east England (med.mean: 0.27, med.max: 0.47),

446 north-west England (med.mean: 0.26, med.max: 0.46), east Scotland (med.mean: 0.21,

447 med.max: 0.39).

448

449

450
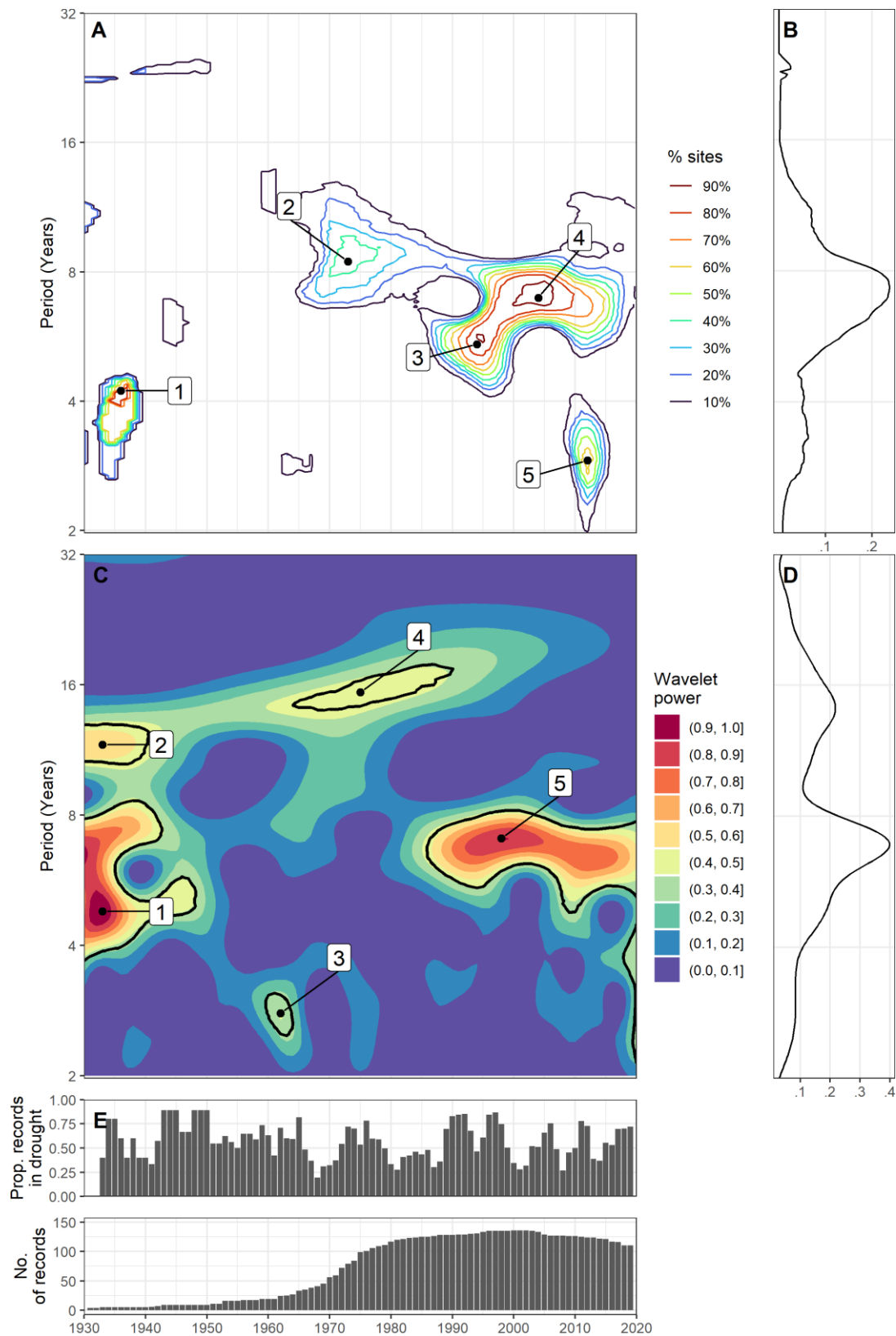
Figure 2 – a) Significance (95% CI) contours between GWL and NAOI, b) time-averaged
proportion of gwl records with a significant XWP with the NAOI (measured as a decimal
fraction), c) wavelet (spectral) power of GWL drought series, d) time-averaged wavelet
(spectral) power of GWL drought series, e) GWL drought coverage time series, f) temporal
coverage of records.

456
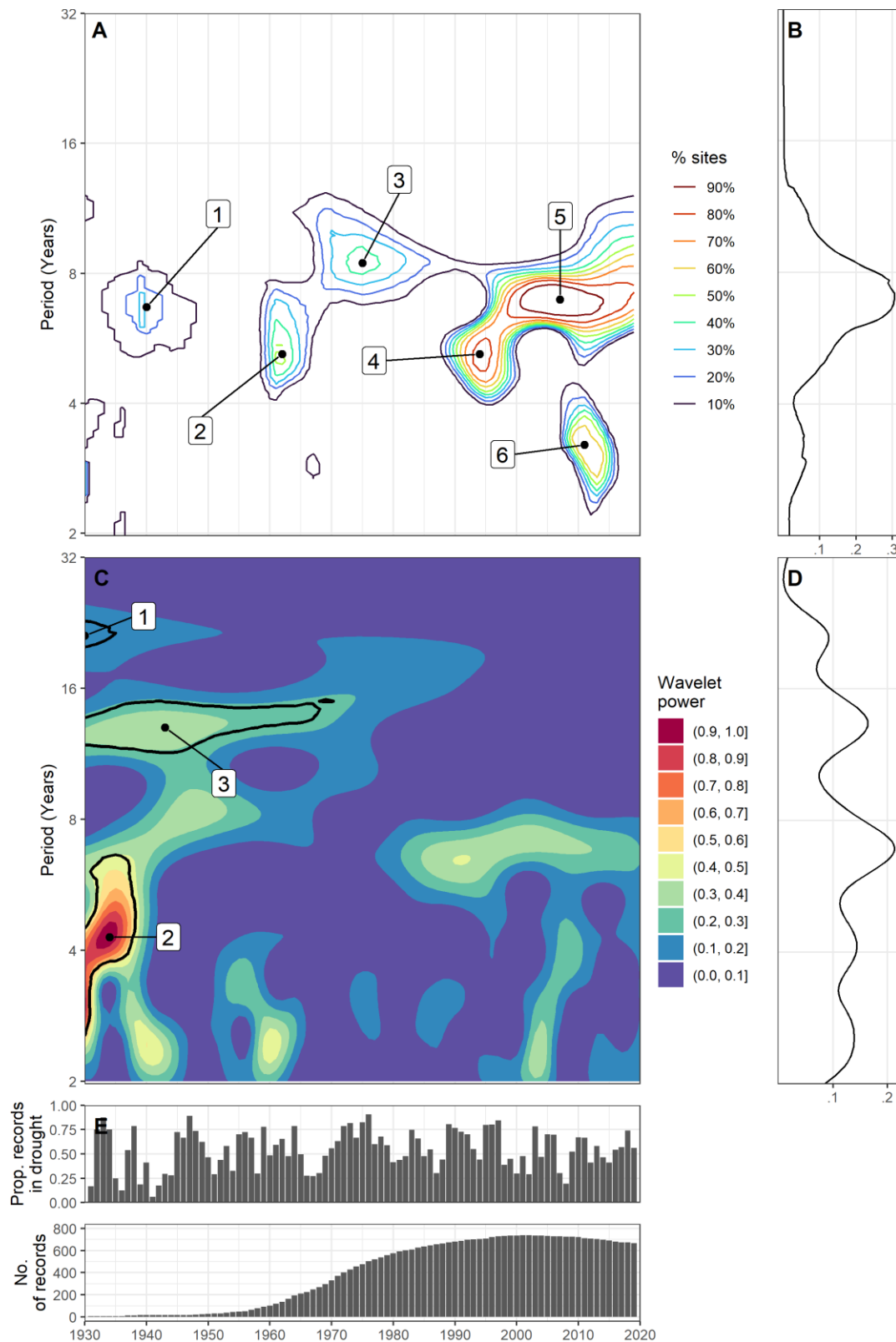
Figure 3 – a) Significance (95% CI) contours between SF and NAOI, b) time-averaged
proportion of SF records with a significant XWP with the NAOI (measured as a decimal
fraction),c) wavelet (spectral) power of SF drought series, d) time-averaged wavelet
(spectral) power of SF drought series, e) SF drought series showing proportion of records in
drought each year, f) temporal coverage of records.

462
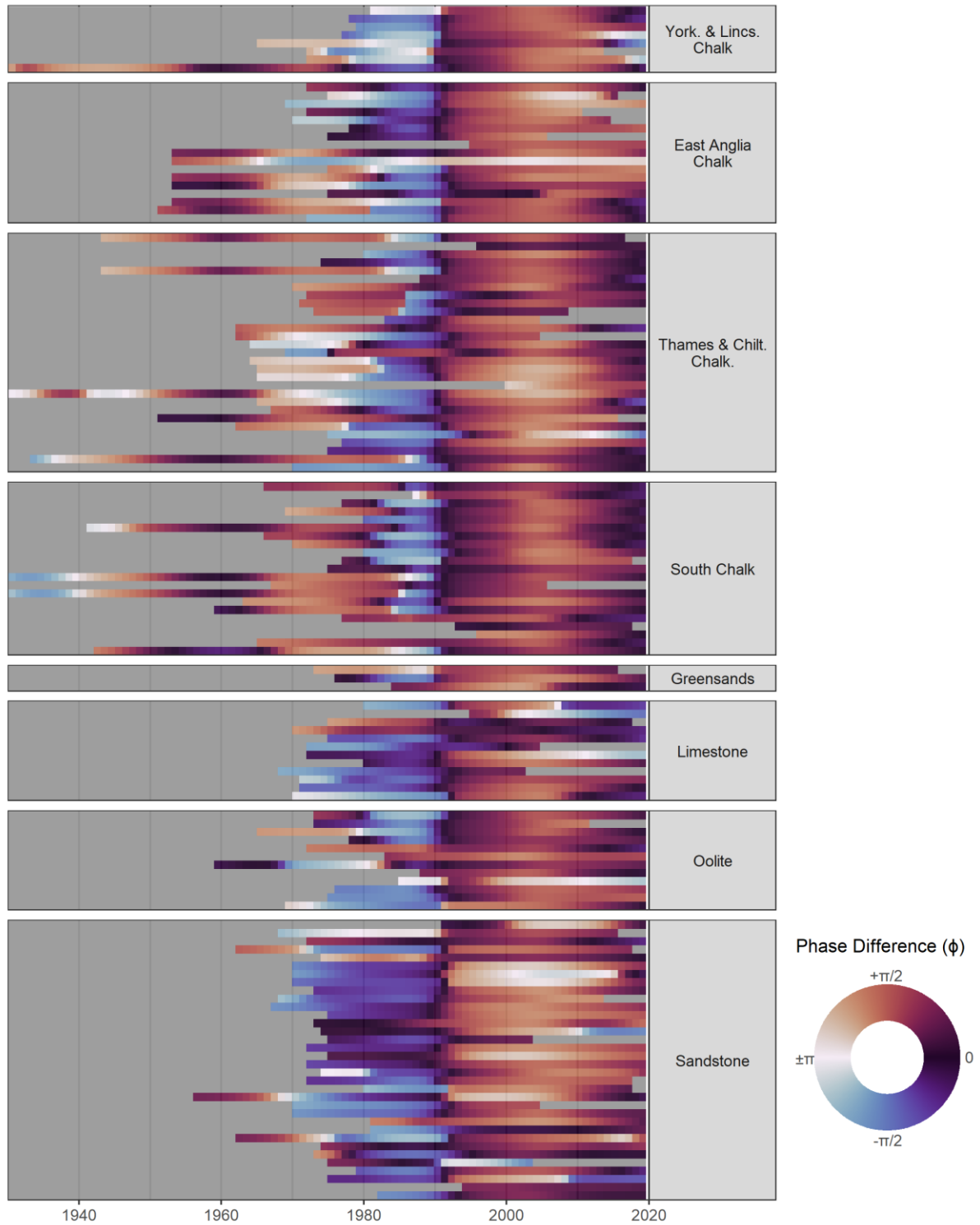
Figure 4 – Phase difference between the NAOI and each GWL record for the GWL record
period. Results are grouped by aquifer regions. ϕ = 0 is equivalent to an in-phase
relationship and ϕ = ±π is equivalent to an antiphase relationship.

466
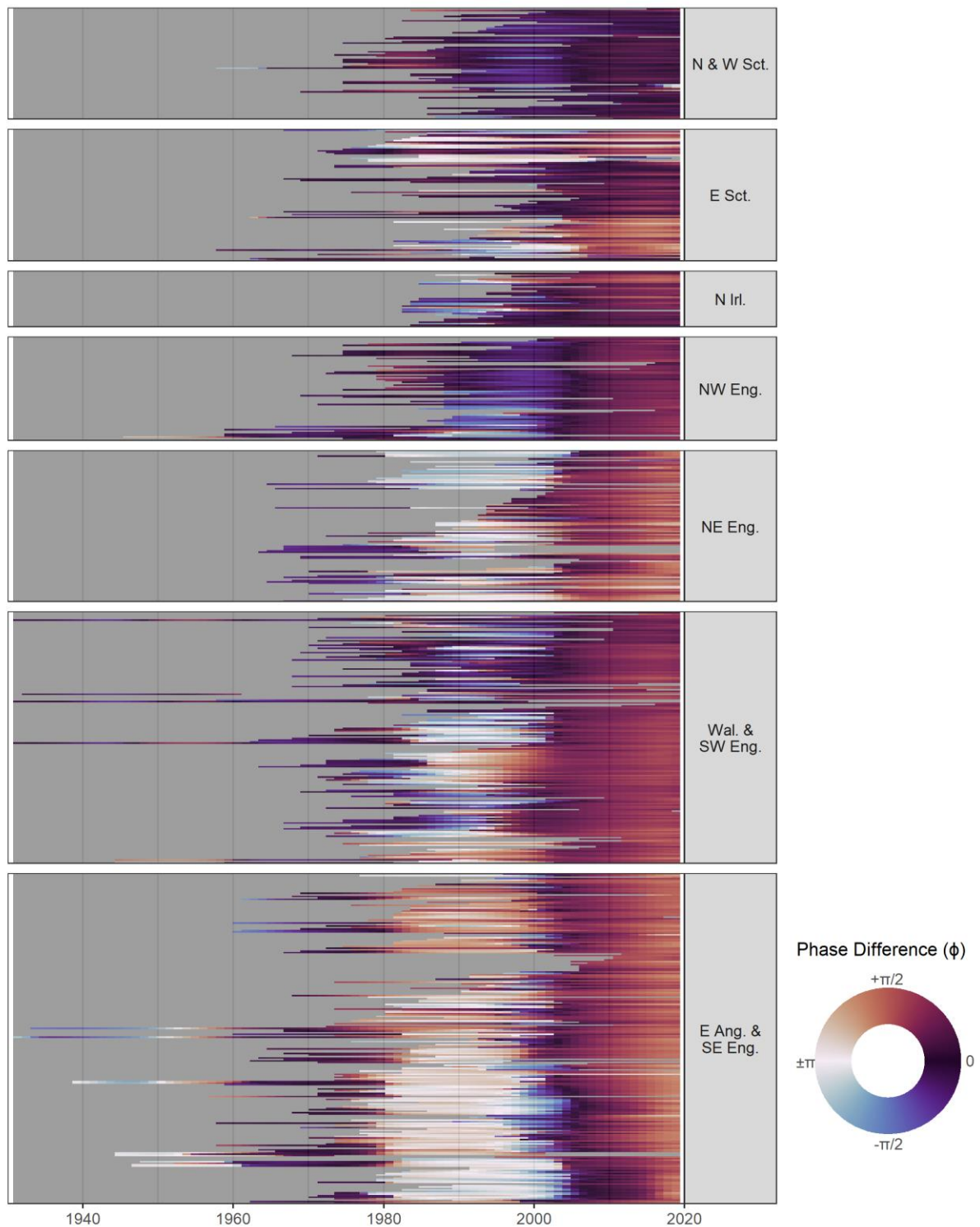
Figure 5 – Phase difference between the NAOI and each streamflow record for the streamflow record period. Results are grouped by regions. ɸ = 0 is equivalent to an in-phase relationship and ɸ = ±π is equivalent to an antiphase relationship.

474
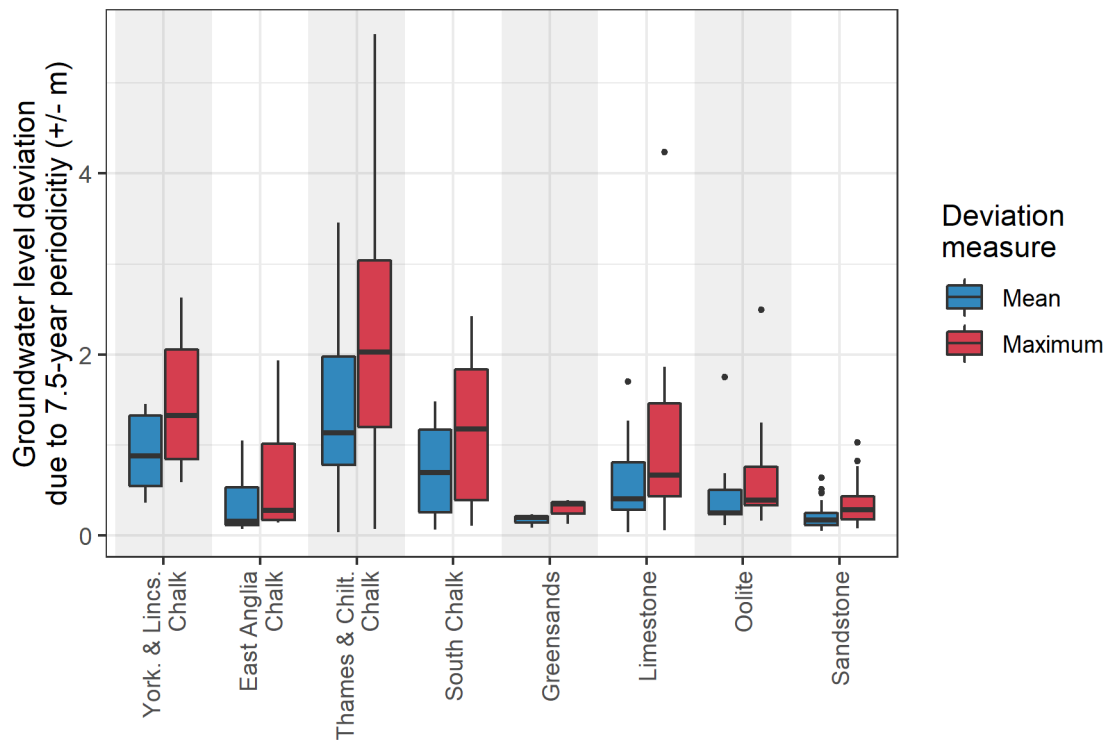
475   Figure 6 – Distribution of absolute mean and maximum modulation of summer groundwater

476   level as a result of the principal cross-wavelet periodicity between the NAOI and winter

477   Groundwater level by aquifer region

478
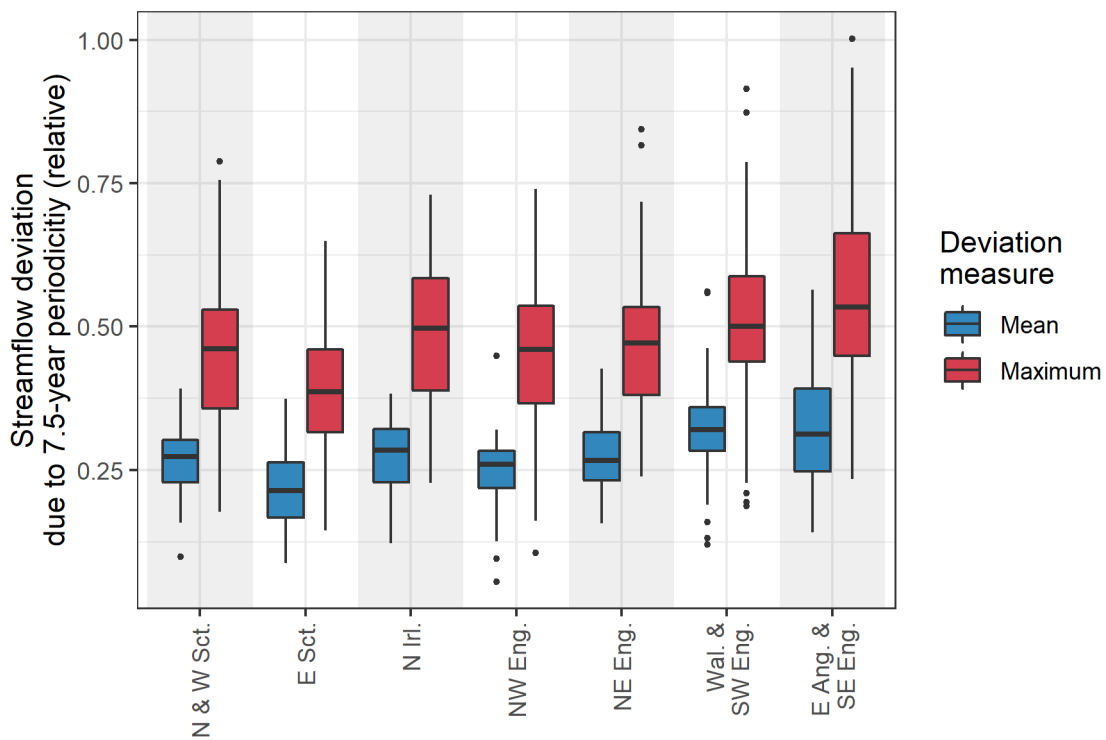
Figure 7 – Modulation of summer streamflow (relative to record standard deviation) as a result of the principal cross-wavelet periodicity between the NAOI and winter streamflow.

5. Discussion

5.1. Historical covariances between the NAOI and water resources at multiannual periodicities

Our results show that the dominant mode of multiannual covariance between the NAOI and UK water resources is at the ~7.5-year periodicity. This is apparent in the time-averaged covariance significance plots for groundwater (figure 2b) and streamflow (figure 3b). The same 7.5-year periodicity is also the strongest average mode of periodic behaviour in water resource drought. Periodicities of similar lengths have previously been detected in European GWL records, such as those in the UK (Rust et al, 2018 Holman et al, 2011), Hungary (Garamhegyi et al, 2016), Spain (Luque-Espinar et al, 2008), Italy (De Vita et al 2011), and Germany (Liesch and Wunsch, 2019); and European streamflow records, for example in the UK (Rust et al 2021; Burt and Howden, 2013) and Sweden (Uvo et al, 2021). Our results therefore are consistent with principal periodicities detected in wider European water resources and highlight the NAO's wide-scale control on water resource drought.

Despite the prominence of the average 7.5-year periodicity in water resource variables, the wider time-frequency spectra show that the NAO's multiannual control on water resources is subject to considerable transience and non-stationarity across time and frequency. For instance, the percentage of water resource records with a significant covariance with the NAOI at the 7.5-year periodicity remains below 10% until between 1960 and 1965, with significance becoming abruptly widespread (> 30%) between 1980 and 1985. As such this suggests that the NAO's control on water resources, at the 7.5-year periodicity, has only been prominent over the past four to five decades. Furthermore, prior to this mode of behaviour, an approximate 16-year periodicity predominated the water resource drought record that did not covary with NAOI. Previous studies have associated a minimum in this 16-year cycle in water resources with the wide-scale 1976 drought (Rust et al, 2019) that

506 affected most UK water resources, particularly in the south of the country (Rodda and

507 Marsh, 2011). These findings are also consistent with Barker et al (2019) who demonstrate

508 longer duration drought events in the UK for the period 1940 to 1980 (approximately), and

509 comparatively shorter drought durations for the period 1980 to present. This may be

510 explained by a more prominent low-frequency influence on water resources and drought

511 during this former period (1940 – 1980), causing longer negative anomalies on drought

512 indices. Finally, Holman et al (2011) linked a 16-year periodic behaviour in groundwater

513 records with the East Atlantic pattern, the second-most dominant mode of atmospheric

514 variability in the North Atlantic region. Our results could be interpreted as suggesting an

515 abrupt shift towards increased frequency of water resource drought around 1970 to 1980 as

516 a result of a transition of periodic control from the EA to the NAO. This interpretation may

517 expand on findings from Neves et al (2019) who demonstrate that historical droughts in

518 southwest Europe are better explained with a combination of NAO and EA influence. It

519 should be noted that, for periodicities of length 20-years or longer (from which a portion of

520 the increased spectral strength around the 16-year periodicity is comprised), confidence in

521 periodicity strength and detection may start to reduce given the 20-year minimum record

522 length used.

523

524 Multiple studies have noted a marked change in European hydrological drought trends since

525 the 1970s, often in the context of the ongoing effects of climate change on water resources

526 (Tanguy et al 2021; Rodda and Marsh, 2011; Bloomfield et al., 2019). These impacts vary

527 depending on the water resource and region but can include changing drought frequency

528 (Spinoni et al, 2015; Bloomfield et al., 2019; Chiang et al, 2021), severity (Hanel et al, 2018;

529 Bloomfield et al., 2019), and increasing divergence of drought characteristic across Europe

530 (Cammalleri et al, 2020). We show here that a dominant 7.5-year periodicity, driven by the

531 NAO, has occurred coincident to these reported changing trends, and proceeded a

532 secondary periodicity of approximately 16 years. As such our results suggest that some of

533   the change in drought frequency that has been noted to have occurred since the 1970s, may

534   be in-part driven by the NAO's increased periodic control on water resources. Hydroclimate

535   studies often highlight that the interaction between climate change, ocean-atmosphere

536   processes and land-surface processes may be complex, resulting in non-linear hydrological

537   responses to increasing global temperatures (Rial et al 2004, Wu et al, 2018). As such, the

538   abrupt emergence of a 7.5-year periodicity between the NAO and water resource drought

539   between 1980 and 1985, and its weaking since 2005, may be evidence of this type of non-

540   linear response. While there have been many studies assessing the impact of climate

541   change projections on the NAO (e.g. Rind et al (2005); Woolings and Blackburn (2012)),

542   there have been few that have investigated potential interactions between climate change

543   and multiannual periodicities in the NAO. As such, the role of climate change in affecting the

544   non-stationary periodicities (detected in this study) is currently unknown.

545   Yuan et al (2017) highlight the importance of suitable calibration period selection for the

546   development of drought early warning systems, particularly in climate change scenarios.

547   Many of these systems in Europe (e.g. Hall and Hanna, 2018; Svensson et al., 2015) rely on

548   high-resolution hydrometeorological datasets for calibration of historical relationships, many

549   of which are only available for recent decades (Rust et al, 2021b, Sun et al 2018). We show

550   here that frequency statistics potentially used as calibration bases for water resource early

551   warning systems can exhibit both multidecadal periods of stability and abrupt sub-decadal

552   non-stationarities, driven by multiannual behaviours in the NAO. Furthermore, we show a

553   weakening of the dominant 7.5-year periodicity since 2005, suggesting a different frequency

554   structure may predominate water resource drought from the 2020s. This further highlights

555   the need for continuous recalibration of critical forecasting utilities, and the potential benefit

556   of including the NAOI as a covariate when understanding multiannual periodic variability in

557   European water resources.

558

5.2. Phase difference between NAO and water resource records at 7.5-year periodicity

The quantification of lead times between meteorological processes and water resource response is critical in the development of early warning systems for water resource management. As such, hydroclimate studies have sought to investigate temporal lags between multiannual periodicities in the NAO and water resource variables across Europe (Uvo et al, 2021, Neves et al 2019, Holman et al 2011). However, previous research has highlighted that the relationship strength and sign between the NAO and European rainfall is non-stationary at sub-decadal to decadal timescales (Rust et al 2021, Vicente-Serrano & López-Moreno, 2008). The extent to which this non-stationarity is projected to multiannual periodicities in water resources was previously unknown. Sign change is synonymous with a phase difference shift of approximately π between periodic components of the NAO and water resources, and as such has the potential to disrupt the projection of lead times into future scenarios. Here we assess the phase difference between the NAO and water resources at a country scale to identify the extent to which this non-stationary is present at multiannual periodicities.

Most water resources records exhibit an abrupt shift in phase difference of approximately -π around 1990. An earlier shift (of approximately +π) is also apparent between 1970 and 1980, however this is less temporally aligned across the fewer records that cover this period. This suggests that, for the period of approximately 1970 to 1990, the relationship sign between the NAO and water resources was inverted. Furthermore, the timing of this period of inversion generally aligns with reported periods of sign inversion in existing studies between the NAO and UK rainfall (Rust et al 2021, Vicente-Serrano & López-Moreno, 2008). It is interesting to note that this period of inversion is notably shorter for some groundwater level records of the Chalk (e.g., those in South Chalk and Thames and Chiltern Chalk). Rust et al (2021) showed the south and south east of the UK was subject to the increased non-stationarity of the NAO-precipitation relationship when compared to other regions, which

586   may explain these relatively short periods of relationship inversion. A similar spatial pattern

587   is shown in the streamflow records, with minimal phase difference shifts in northwest

588   England, Scotland, and Northern Ireland where more stable signs have been found by Rust

589   et al (2021b).

590   Localisation of this non-stationarity between the NAO and water resources at multiannual

591   periodicities suggests it is possible to identify a discrete time period of sufficient stationarity

592   from which to calculate lead-in times for early warning systems (for instance, between 1990

593   and 2020). However, phase differences for this period also show a degree of non-

594   stationarity, varying by up to approximately $\pm\frac{1}{4}\pi$. Some of this variance may be due to

595   changing storage dynamics within a catchment over time (Rust et al, 2014; Beverly and

596   Hocking, 2012), but also the introduction of red noise from reconstructing from non-

597   significant wavelets. This also explains the increased variance seen in aquifer groups

598   characterised by higher autocorrelation (e.g., Sandstone) (Bloomfield and Marchant, 2013),

599   and the relatively low variance seen in streamflow records which often have lower

600   autocorrelation when compared to groundwater level (Hannaford et al, 2021).   While this

601   can be minimised by calculating phase difference from significant wavelets only, we have

602   shown in the previous section that the significance between the NAO and water resources

603   and multiannual periodicities is also subject to notable non-stationarity.

604   Finally, in order to calculate accurate lead-in times between periodicities in the NAO and

605   water resources in future scenarios, a sufficient systematic understanding of the NAO sign

606   non-stationarity is required. However, there is limited research that has investigated the

607   causes for these modes of multiannual non-stationarity. Vicente-Serrano & López-

608   Moreno (2008) suggest that an eastward shift of the NAO's southern centre of action may

609   account for a portion of this variability, but highlight that further work is required for this to be

610   a sufficient explanation of a changing correlation between the NAO and European rainfall.

611   As such, existing non-stationarities between the NAO and water resources at multiannual

612   periodicities remains a considerable barrier to its application in improving preparedness for

613   future water resource drought.

5.3.   NAO multiannual modulations on water resources in future scenarios

615   Water resource management systems are in place across Europe to improve planning and

616   preparedness for the projected effects of climate change. As such, in order for multiannual

617   NAO modulations of water resources to have sufficient utility for water management systems

618   in future scenarios, they need to exhibit a comparable influence on water resources to the

619   projected effects of climate change. Here, we present historical modulations of summer

620   water resource variables from the principal NAO periodicity alongside expected impacts on

621   water resources from climate change projections in order to discuss their comparative

622   influence.

623   Jackson et al (2015) estimated median groundwater level change due to climate change in

624   24 boreholes across Chalk, limestone, sandstone and greensand aquifer groups in the UK

625   for the 2050s under a high emission scenario for September (as a typical annual minima of

626   groundwater levels in the UK). Median level from each site in Jackston et al (2015) have

627   been regrouped and averaged across the broad aquifer groups used in this study to allow

628   comparison with historical deviations in water resource results as a result of the NAO's 7.5-

629   year periodicity. This comparison is provided in Table 1. A mapping table of this comparison

630   is available in the supplementary material.

631

Aquifer group	50th %ile gwl change due to climate change (m)	Gwl deviation due to 7.5-year NAO periodicity (± m) (med.mean)	Gwl deviation due to 7.5-year NAO periodicity (± m) (med.max)
Chalk (East Anglia)	-0.21	0.16	0.31
Chalk (Lincolnshire)	-0.31	0.71	1.03
Chalk (South)	-0.64	0.73	1.08
Chalk (Thames / Chilterns)	-0.69	0.86	1.33
Limestone	-0.28	0.35	0.51
Oolite	-0.36	0.21	0.33
Sandstone	-0.07	0.15	0.25
Greensands	-0.10	0.12	0.17

632 Table 1 – synthesis of Table 3 from Jackson et al (2015). Median results from the absolute
633 teleconnection modulation on groundwater level from Figure 3 of this paper are also
634 presented for the mean and maximum modulation cases. NAO teleconnection modulations
635 greater than the reported 50th percentile climate change modulation are shaded in grey.
636
637
638 Historical modulations in groundwater level due to multiannual periodicities in the NAO were

639 greater than projected GWL modulation from a high emissions climate change scenario, in

640 all but two aquifer groups for mean NAO modulation (East Anglia Chalk, Oolite), and all but

641 one for maximum NAO modulation (Oolite). Similar degrees of GWL modulation from climate

642 change scenarios have been shown for wider European aquifer systems (e.g., Dams et al,

643 2011), and our results for NAO modulations of GWL are of a similar degree to those reported

644 by Neves et al (2019) for aquifers in the Iberian Peninsula. While few studies have looked at

645 multiannual NAO modulations of groundwater level across Europe, our results here suggest

646 a similar response across Western Europe, where the NAO has a greater influence on

647 precipitation (Trigo et al, 2002). However, existing studies notable uncertainties in the future

648 trends of groundwater level change due to climate change. For instance, Yusoff et al. (2002)

649 demonstrated that it was not possible to predict whether groundwater level would rise or fall

650 between 2020s and 2050s, Bloomfield et al. (2003) showed that groundwater levels were

651 expected to rise in the 2020s but fall in the 2050s, and, Jackson et al (2015) showed

652 reductions in annual and average summer levels but increases in average winter levels by

653 the 2050s. For streamflow, Kay et al (2020) give estimated modulations to low flows (Q95)

654 as a result of climate change (2050 horizon). While no Scottish catchments were used in the

655 study, percentage modulations for low flows were found to be mostly between 0 to -20%

656 change with some catchments showing up to -40% change for catchments in the West and

657 South West of the UK. Schnieder et al (2013) show similar low flow modulations across

658 Europe as a result of climate change, ranging from +20% for northwest Europe to -40% in

659 the Iberian Peninsula. As such, our results for streamflow (Figure 7) indicate that multiannual

660 NAO modulation of streamflow has been, on average, comparable to the expected change

661 due to climate change scenarios. NAO modulations in streamflow are notably less than

662 those found in groundwater level, as may be expected given the established sensitivity of

663 groundwater processes to long-term changes in meteorological fluxes (Forootan et al., 2018;

664 Van Loon, 2015; Folland et al., 2015). Given the scale of multiannual NAO influence on

665 water resource compared to the estimated effects of climate change, the NAO may have the

666 potential to impact the projected trend of water resource variability in certain future scenarios

667 more than was previously understood, and therefore effect the required adaptive

668 management response. However, existing research has shown that that current GCMs do

669 not fully replicate low frequency behaviours in the NAO that have been historical recorded

670 (Eade et al, 2021). Given the importance of multiannual periodicities the NAO in defining

671 water resource behaviour, demonstrated here and in other research (e.g., Uvo et al, 2021;

672 Neves et al, 2019), this raises notable uncertainties in the use of GCMs outputs for

673 projecting European water resource behaviour into future scenarios. Findings reported here

674 suggest that current projections from these GCMs may contain error that is comparable to

675 the current projected effect of climate change on water resources. This therefore highlights

676 the need for improved low frequency representation in GCMs, and for an understanding of

677 the non-stationary atmospheric behaviours are can considerably influence wide-scale water

678 resource behaviour.

679 It is important to note , given the large number of sites used from the NRFA in this study, that

680 no consideration has been made here for the role of anthropogenic influence on catchment

681 response. We acknowledge here that, depending on the way in which river management

682 regimes are applied, water resources frequencies may be altered or compounded by

683 anthropogenic. However, it is expected that, in the majority of cases, these influences (e.g.,

684 effluent discharge or managed streamflow regimes) may produce a noise within the

685 frequency spectra of streamflow, but not impart a systematic periodicity. Furthermore, while

686 studies have detected the influence of climate-induced abstraction (Wendt et al, 2020;

687 Gurdak, 2017), these influences have generally been small in comparison to the driving

688 drought anomalies. As such we expect anthropogenic influences to have a minimal effect on

689 the findings of this study. It is suggested that the role of anthropogenic influences on UK

690 water resources frequency spectra is investigated as part of future research.

691 Additionally, while this study focuses on UK water resources, 132 of the 136 groundwater

692 boreholes used are located in England with the majority of these situated within the Chalk.

693 While this skew does not affect the findings of this paper, it is important to note that broad-

694 scale multiannual periodicities of groundwater resources in Wales, Northern Ireland or

695 Scotland have not been assessed here.

696 Rust et al (2018) set out a conceptual model for how multiannual modulations of water

697 resources due to the NAO may provide a system for improving water resource forecasts and

698 management regimes. This model highlights the need for a systematic understanding of how

699 multiannual periodicities affect water resources over time, including temporal lags and

700 amplitude modulation between the NAO and water resources. We demonstrate that the

701 degree to which the NAO's 7.5-year periodicity has modulated historical water resources is

702 of a similar order of magnitude to the estimated impacts on water resource variables from

703 climate change projections. These results further show the importance of including the

704 influence of multiannual NAO periodicities on water resources in the understanding of future

705 drought, as they have the potential to affect the required management regime for certain

706 resources in climate change scenarios. However, we also show that there are notable non-

707 stationarities in NAO periodicities over time and their relationship with water resource

708 response, for which there is limited systematic understanding in existing hydroclimate

709 literature.

710

6. Conclusions

712 This paper assesses the utility of the relationship between the NAO and water resources, at

713 multiannual periodicities, for improving preparedness of water resource drought in Europe.

714 We review this relationship in the context of non-stationary dynamics within the NAO and its

715 control on UK meteorological variables, as well as its potential impact on water resources in

716 climate change scenarios. We provide new evidence for the time-frequency relationship

717 between the NAO and water resources in western Europe showing that a wide-spread 7.5-

718 year periodicity, which predominates the multiannual frequency structure of many European

719 water resources, is the result of a non-stationary control from the NAO between

720 approximately 1970 and 2020. Furthermore, we show that known non-stationarities of the

721 relationship sign between the NAOI and European rainfall at the annual scale are present in

722 water resources at multiannual scales. A current lack of systematic understanding of both

723 these forms of non-stationarity, in existing atmospheric or meteorological literature, is a

724 considerable barrier to the application of this multiannual relationship for improving

725 preparedness for future water resource drought. However, we also show that the degree of

726 modulation from multiannual NAO periodicities on water resources can be comparable to

727 modulations from a worst-case climate change scenario. As such multiannual periodicities

728 offer a valuable explanatory variable for ongoing water resource behaviour that have the

729 potential to heavily impact the required management regimes for individual resources in

730 climate change scenarios. Therefore, we highlight knowledge gaps in atmospheric research

731 (e.g. the ability of climate models to simulate NAO non-stationarities) that need to be

732 addressed in order for multiannual NAO periodicities to be used in improving early warning

733 systems or improving preparedness for water resource drought.

734 **Data availability.**

735 The groundwater level data used in the study are from the WellMaster Database in the

736 National Groundwater Level Archive of the British Geological Survey. The data are available

737 under license from the British Geological Survey at https:

738 //www.bgs.ac.uk/products/hydrogeology/WellMaster.html (last accessed: 24/10/2021).

739 The streamflow data as well as the metadata used in this study are freely available at the

740 NRFA website at http://nrfa.ceh.ac.uk/ (last accessed: 25/10/2021).

741 The data that support the findings of this study are available in Cranfield Online Research

742 Data (CORD) at 10.17862/cranfield.rd.16866868. This study was a re-analysis of existing

743 data that are publicly available from NCAR at https://climatedataguide.ucar.edu/climate-data.

744

745 **Author contributions.**

746 WR designed the methodology and carried them out with supervision from all co-authors. WR

747 prepared the article with contributions from all co-authors.

748 **Competing interests.**

749 The authors declare that they have no conflict of interest.

750

751 **Acknowledgements.**

752 This work was supported by the Natural Environment Research Council (grant numbers

753 NE/M009009/1 and NE/L010070/1) and the British Geological Survey (Natural Environment

754 Research Council). JPB publishes with the permission of the Executive Director, British

755 Geological Survey (NERC). MOC gratefully acknowledges funding for an Independent

756   Research Fellowship from the UK Natural Environment Research Council (NE/P017819/1).

757   We thank Angi Rosch and Harald Schmidbauer for making their wavelet package

758   "WaveletComp" freely available.

759

760   **Financial support.**

761   This research has been supported by the Natural Environment Research Council (grant nos.

762   NE/M009009/1 and NE/L010070/1), and MOC has been supported by an Independent

763   Research Fellowship from the UK Natural Environment Research Council (NE/P017819/1).

764

765   **References**

766   Allen, D.J., Brewerton, L.J., Coleby, L.M., Gibbs, B.R., Lewis, M.A., MacDonald, A.M.,

767   Wagstaff, S.J., Williams, A.T.: The physical properties of major aquifers in England and

768   Wales. British Geological Survey, 333pp, BGS Report WD/97/034,

769   http://nora.nerc.ac.uk/id/eprint/13137/, 1997,

770   Allen, M. R., Smith, L. A., Allen, M. R., and Smith, L. A.: Monte Carlo SSA: Detecting

771   irregular oscillations in the Presence of Colored Noise, J. Clim., 9, 3373–3404,

772   https://doi.org/10.1175/1520-0442(1996)009<3373:MCSDIO>2.0.CO;2, 1996.

773   Beverly, C. and Hocking, M.: Predicting Groundwater Response Times and Catchment

774   Impacts From Land Use Change, Australasian Journal of Water Resources, 16, 29–47,

775   https://doi.org/ 10.7158/13241583.2012.11465402, 2012.

776   Bloomfield, J.P.: The role of diagenesis in the hydrogeological stratification of carbonate

777   aquifers: An example from the Chalk at Fair Cross, Berkshire, UK, Hydrol. Earth Sys. Sci.,,

778   1, 19-33, https://doi.org/10.5194/hess-1-19-1997 , 1997.

779 Bloomfield, J. P., Gaus, I., and Wade, S. D.: A method for investigating the potential impacts

780 of climate-change scenarios on annual minimum groundwater levels,

781 https://doi.org/10.1111/j.1747-6593.2003.tb00439.x, 2003.

782 Bloomfield, J. P. and Marchant, B. P.: Analysis of groundwater drought building on the

783 standardised precipitation index approach, Hydrol. Earth Syst. Sci., 17, 4769–4787,

784 https://doi.org/10.5194/hess-17-4769-2013 , 2013.

785 Bloomfield, J.P., Marchant, B.J., and McKenzie, A.A.:2019. Changes in groundwater drought

786 associated with anthropogenic warming, Hydrol. Earth Syst. Sci., 23, 1393–1408,

787 https://doi.org/10.5194/hess-23-1393-2019, 2019.

788 Bonaccorso, B., Cancelliere, A., and Rossi, G.: Probabilistic forecasting of drought class

789 transitions in Sicily (Italy) using Standardized Precipitation Index and North Atlantic

790 Oscillation Index, J. Hydrol., 526, 136–150, http://dx.doi.org/10.1016/j.jhydrol.2015.01.070,

791 2015

792 Brady, A., Faraway, J., and Prosdocimi, I.: Attribution of long-term changes in peak river

793 flows in Great Britain, Hydrol. Sci. J., 64, 1159–1170,

794 https://doi.org/10.1080/02626667.2019.1628964, 2019.

795 Burt, T. P. and Howden, N. J. K.: North Atlantic Oscillation amplifies orographic precipitation

796 and river flow in upland Britain, Water Resour. Res., 49, https://doi.org/10.1002/wrcr.20297,

797 2013.

798 Cammalleri, C., Naumann, G., Mentaschi, L., Bisselink, B., Gelati, E., De Roo, A., and

799 Feyen, L.: Diverging hydrological drought traits over Europe with global warming, Hydrol.

800 Earth Syst. Sci., 24, 5919–5935, https://doi.org/10.5194/hess-24-5919-2020, 2020.

801 Chiang, F., Mazdiyasni, O., and AghaKouchak, A.: Evidence of anthropogenic impacts on

802 global drought frequency, duration, and intensity, Nat. Commun., 12, 2754,

803 https://doi.org/10.1038/s41467-021-22314-w, 2021.

Coleman, J. S. M. and Budikova, D.: Eastern U.S. summer streamflow during extreme phases of the North Atlantic oscillation, J. Geophys. Res., 118, 4181–4193, http://dx.doi.org/10.1002/jgrd.50326, 2013.

Dams, J., Salvadore, E., Van Daele, T., Ntegeka, V., Willems, P., and Batelaan, O.: Spatio-temporal impact of climate change on the groundwater system, Hydrol. Earth Syst. Sci., 16, 1517–1531, https://doi.org/10.5194/hess-16-1517-2012, 2012.

Deser, C., Hurrell, J. W., and Phillips, A. S.: The role of the North Atlantic Oscillation in European climate projections, Clim. Dyn., 49, 3141–3157, https://doi.org/10.1007/s00382-016-3502-z, 2017.

De Vita, P., Allocca, V., Manna, F., and Fabbrocino, S.: Coupled decadal variability of the North Atlantic Oscillation, regional rainfall and karst spring discharges in the Campania region (southern Italy), Hydrol. Earth Syst. Sci., 16, 1389–1399, https://doi.org/10.5194/hess-16-1389-2012, 2012.

Dixon, H., Hannaford, J., and Fry, M. J. The effective management of national hydrometric data: experiences from the United Kingdom, Hydrological Sciences Journal, 58:7, 1383-1399, DOI: 10.1080/02626667.2013.787486. 2013

Feng, P.-N., Lin, H., Derome, J., and Merlis, T. M.: Forecast Skill of the NAO in the Subseasonal-to-Seasonal Prediction Models, J. Clim., 34, 4757–4769, https://doi.org/10.1175/JCLI-D-20-0430.1, 2021.

Folland, C. K., Hannaford, J., Bloomfield, J. P., Kendon, M., Svensson, C., Marchant, B. P., Prior, J., and Wallace, E.: Multi-annual droughts in the English Lowlands: a review of their characteristics and climate drivers in the winter half-year, Hydrol. Earth Syst. Sci., 19, 2353–2375, https://doi.org/10.5194/hess-19-2353-2015, 2015.

Forootan, E., Khaki, M., Schumacher, M., Wulfmeyer, V., Mehrnegar, N., van Dijk, A. I. J. M., Brocca, L., Farzaneh, S., Akinluyi, F., Ramillien, G., Shum, C. K., Awange, J., and

829   Mostafaie, A.: Understanding the global hydrological droughts of 2003–2016 and their

830   relationships with teleconnections, Sci. Total Environ.,

831   https://doi.org/10.1016/J.SCITOTENV.2018.09.231, 2018.

832   Gao, L., Deng, Y., Yan, X., Li, Q., Zhang, Y., and Gou, X.: The unusual recent streamflow

833   declines in the Bailong River, north-central China, from a multi-century perspective, Quat.

834   Sci. Rev., 260, 106927, http://dx.doi.org/10.1016/j.quascirev.2021.106927, 2021.

835   Garamhegyi, T., Kovács, J., Pongrácz, R., Tanos, P., and Hatvani, I. G.: Investigation of the

836   climate-driven periodicity of shallow groundwater level fluctuations in a Central-Eastern

837   European agricultural region, Hydrogeol. J., 26, 677–688, https://doi.org/10.1007/s10040-

838   017-1665-2, 2018.

839   Gurdak, J. J.: Climate-induced pumping, Nat. Geosci., 10, 71–71, 2017.

840   Hanel, M., Rakovec, O., Markonis, Y., Máca, P., Samaniego, L., Kyselý, J., and Kumar, R.:

841   Revisiting the recent European droughts from a long-term perspective, Sci. Rep., 8, 9499,

842   https://doi.org/10.1038/s41598-018-27464-4, 2018.

843   Holman, I., Rivas-Casado, M., Bloomfield, J. P., and Gurdak, J. J.: Identifying non-stationary

844   groundwater level response to North Atlantic ocean-atmosphere teleconnection patterns

845   using wavelet coherence, Hydrogeol. J., 19, 1269–1278, https://doi.org/10.1007/s10040-

846   011-0755-9, 2011.

847   Hurrell, J. W., Kushnir, Y., Ottersen, G., and Visbeck, M.: An Overview of the North Atlantic

848   Oscillation, in: The North Atlantic Oscillation: Climatic Significance and Environmental

849   Impact, American Geophysical Union, 1–35, https://doi.org/10.1029/GM134 2003.

850   Hurrell, J. W.: Decadal trends in the north atlantic oscillation: regional temperatures and

851   precipitation, Science, 269, 676–679, https://doi.org/10.1126/science.269.5224.676, 1995.

852   Hurrell, J. W. and Deser, C.: North Atlantic climate variability: The role of the North Atlantic

853   Oscillation, J. Mar. Syst., 79, 231–244, https://doi.org/10.1016/j.jmarsys.2008.11.026, 2010.

854   Jackson, C. R., Bloomfield, J. P., and Mackay, J. D.: Evidence for changes in historic and

855   future groundwater levels in the UK, Prog. Phys. Geogr., 39, 49–67,

856   https://doi.org/10.1177%2F0309133314550668, 2015.

857   Kay, A. L., Watts, G., Wells, S. C., and Allen, S.: The impact of climate change on U. K. river

858   flows: A preliminary comparison of two generations of probabilistic climate projections,

859   Hydrol. Process., 34, 1081–1088, https://doi.org/10.1002/hyp.13644, 2020.

860   Konapala, G., Mishra, A. K., Wada, Y., and Mann, M. E.: Climate change will affect global

861   water availability through compounding changes in seasonal precipitation and evaporation,

862   Nat. Commun., 11, 3044, https://doi.org/10.1038/s41467-020-16757-w, 2020.

863   Kingston, D. G., McGregor, G. R., Hannah, D. M., and Lawler, D. M.: River flow

864   teleconnections across the northern North Atlantic region, Geophys. Res. Lett., 33, 1–5,

865   http://dx.doi.org/10.1029/2006GL026574, 2006.

866   Kuss, A. M. and Gurdak, J. J.: Groundwater level response in U.S. principal aquifers to

867   ENSO, NAO, PDO, and AMO, J. Hydrol., 519, 1939–1952,

868   https://doi.org/10.1016/j.jhydrol.2014.09.069, 2014.

869   Labat, D.: Cross wavelet analyses of annual continental freshwater discharge and selected

870   climate indices, J. Hydrol., 385, 269–278, https://doi.org/10.1016/j.jhydrol.2010.02.029,

871   2010.

872   Liesch, T. and Wunsch, A.: Aquifer responses to long-term climatic periodicities, J. Hydrol.,

873   572, 226–242, http://dx.doi.org/10.1016/j.jhydrol.2019.02.060, 2019.

874   Luque-Espinar, J. A., Chica-Olmo, M., Pardo-Igúzquiza, E., and García-Soldado, M. J.:

875   Influence of climatological cycles on hydraulic heads across a Spanish aquifer, J. Hydrol.,

876   354, 33–52, https://doi.org/10.1016/j.jhydrol.2008.02.014, 2008.

877   Marchant, B.P., and Bloomfield, J.P.: Spatio-temporal modelling of the status of groundwater

878   droughts, J. Hydrol., 564, 397-413, https://doi.org/10.1016/j.jhydrol.2018.07.009, 2018.

879   Marsh, T. and Hannaford, J.: UK Hydrometric Register. Hydrological data UK series, Centre

880   for Ecology and Hydrology, 2008.

881   Meinke, H., deVoil, P., Hammer, G. L., Power, S., Allan, R., Stone, R. C., Folland, C., and

882   Potgieter, A.: Rainfall variability of decadal and longer time scales: Signal or noise?, J. Clim.,

883   18, 89–90, https://doi.org/10.1175/JCLI-3263.1, 2005.

884   Naumann, G., Spinoni, J., Vogt, J. V., and Barbosa, P.: Assessment of drought damages

885   and their uncertainties in Europe, Environ. Res. Lett., 10, 124013,

886   http://dx.doi.org/10.1088/1748-9326/10/12/124013, 2015.

887   Neves, M. C., Jerez, S., and Trigo, R. M.: The response of piezometric levels in Portugal to

888   NAO, EA, and SCAND climate patterns, J. Hydrol., 568, 1105–1117,

889   http://dx.doi.org/10.1016/j.jhydrol.2018.11.054, 2019.

890   Peters, E. Propagation of drought through groundwater systems - illustrated in the Pang

891   (UK) and Upper-Guadiana (ES) catchments. Ph. D. thesis, Wageningen University. 2003

892   Rial, J. A., Pielke, R. A., Sr, Beniston, M., Claussen, M., Canadell, J., Cox, P., Held, H., de

893   Noblet-Ducoudré, N., Prinn, R., Reynolds, J. F., and Salas, J. D.: Nonlinearities, feedbacks

894   and critical thresholds within the earth's climate system, Clim. Change, 65, 11–38,

895   https://doi.org/10.1023/B:CLIM.0000037493.89489.3f, 2004.

896   Rodda, J. and Marsh, T.: The 1975-76 Drought - a contemporary and retrospective review,

897   Centre for Ecology & Hydrology, 2011.

898   Rosch, A. and Schmidbauer, H.: WaveletComp 1.1: a guided tour through the R package,

899   2018.

900   Rust, W., Bloomfield, J. P., Cuthbert, M. O., Corstanje, R., and Holman, I. P.: Non-stationary

901   control of the NAO on European rainfall and its implications for water resource management,

902   Hydrol. Process., 35, https://doi.org/10.1002/hyp.14099, 2021b.

903 Rust, W., Corstanje, R., Holman, I. P., and Milne, A. E.: Detecting land use and land

904 management influences on catchment hydrology by modelling and wavelets, J. Hydrol., 517,

905 378–389, 2014.

906 Rust, W., Cuthbert, M., Bloomfield, J., Corstanje, R., Howden, N., and Holman, I.: Exploring

907 the role of hydrological pathways in modulating multi-annual climate teleconnection

908 periodicities from UK rainfall to streamflow, Hydrol. Earth Syst. Sci., 25, 2223–2237,

909 https://doi.org/10.1016/j.jhydrol.2014.05.052, 2021a.

910 Rust, W., Holman, I., Bloomfield, J., Cuthbert, M., and Corstanje, R.: Understanding the

911 potential of climate teleconnections to project future groundwater drought, Hydrol. Earth

912 Syst. Sci., 23, 3233–3245, https://doi.org/10.5194/hess-23-3233-2019, 2019.

913 Rust, W., Holman, I., Corstanje, R., Bloomfield, J., and Cuthbert, M.: A conceptual model for

914 climatic teleconnection signal control on groundwater variability in Europe, Earth-Sci. Rev.,

915 177, 164–174, https://doi.org/10.1016/j.earscirev.2017.09.017, 2018.

916 Sang, Y.-F.: A review on the applications of wavelet transform in hydrology time series

917 analysis, Atmos. Res., 122, 8–15, https://doi.org/10.1016/j.atmosres.2012.11.003, 2013.

918 Schneider, C., Laizé, C. L. R., Acreman, M. C., and Flörke, M.: How will climate change

919 modify river flow regimes in Europe?, Hydrol. Earth Syst. Sci., 17, 325–339,

920 https://doi.org/10.5194/hess-17-325-2013, 2013.

921 Sun, Q., Miao, C., Duan, Q., Ashouri, H., Sorooshian, S., and Hsu, K.: A review of global

922 precipitation data sets: Data sources, estimation, and intercomparisons, Rev. Geophys., 56,

923 79–107, https://doi.org/10.1002/2017RG000574, 2018.

924 Sutanto, S. J., Van Lanen, H. A. J., Wetterhall, F., and Llort, X.: Potential of Pan-European

925 Seasonal Hydrometeorological Drought Forecasts Obtained from a Multihazard Early

926 Warning System, Bull. Am. Meteorol. Soc., 101, E368–E393, https://doi.org/10.1175/BAMS-

927 D-18-0196.1 , 2020.

928   Svensson, C., Brookshaw, A., Scaife, A. A., Bell, V. A., Mackay, J. D., Jackson, C. R.,

929   Hannaford, J., Davies, H. N., Arribas, A., and Stanley, S.: Long-range forecasts of UK winter

930   hydrology, Environ. Res. Lett., 10, 064006, http://dx.doi.org/10.1088/1748-9326/10/6/064006

931   2015.

932   Tremblay, L., Larocque, M., Anctil, F., and Rivard, C.: Teleconnections and interannual

933   variability in Canadian groundwater levels, J. Hydrol., 410, 178–188,

934   https://doi.org/10.1016/j.jhydrol.2011.09.013, 2011.

935   Trigo, R. M., Osborn, T. J., and Corte-real, J. M.: The North Atlantic Oscillation influence on

936   Europe: climate impacts and associated physical mechanisms, Clim. Res., 20, 9–17,

937   http://dx.doi.org/10.3354/cr020009, 2002.

938   Tanguy, M., Haslinger, K., Svensson, C., Parry, S., Barker, L. J., Hannaford, J., and

939   Prudhomme, C.: Regional Differences in Spatiotemporal Drought Characteristics in Great

940   Britain, Front. Environ. Sci. Eng. China, 9, 67, https://doi.org/10.3389/fenvs.2021.639649,

941   2021.

942   Uvo, C. B., Foster, K., and Olsson, J.: The spatio-temporal influence of atmospheric

943   teleconnection patterns on hydrology in Sweden, 34, 100782,

944   http://dx.doi.org/10.1016/j.ejrh.2021.100782, 2021.

945   Velasco, E. M., Gurdak, J. J., Dickinson, J. E., Ferré, T. P. A., and Corona, C. R.:

946   Interannual to multidecadal climate forcings on groundwater resources of the U.S. West

947   Coast, https://doi.org/10.1016/j.ejrh.2015.11.018, 2015.

948   Van Loon, A.F. On the propagation of drought: How climate and catchment characteristics

949   influence hydrological drought development and recovery. PhD thesis Wageningen

950   University. 2013.

951   Vicente-Serrano, S. M. and López-Moreno, J. I.: Differences in the non-stationary influence

952   of the North Atlantic Oscillation on European precipitation under different scenarios of

953   greenhouse gas concentrations, https://doi.org/10.1029/2008gl034832, 2008.

954   Van Loon, A. F.: Hydrological drought explained, WIREs Water, 2, 359–392,

955   https://doi.org/10.1002/wat2.1085, 2015.

956   Wendt, D. E., Van Loon, A. F., Bloomfield, J. P., and Hannah, D. M.: Asymmetric impact of

957   groundwater use on groundwater droughts, Hydrol. Earth Syst. Sci., 24, 4853–4868,

958   https://doi.org/10.5194/hess-24-4853-2020, 2020

959   West, H., Quinn, N., and Horswell, M.: The Influence of the North Atlantic Oscillation and East

960   Atlantic Pattern on Drought in British Catchments, Front. Environ. Sci. Eng. China, 10,

961   https://doi.org/10.3389/fenvs.2022.754597, 2022.

962   Wrzesiński, D. and Paluszkiewicz, R.: Spatial differences in the impact of the North Atlantic

963   Oscillation on the flow of rivers in Europe, 42, 30–39, https://doi.org/10.2166/nh.2010.077,

964   2011.

965   Wu, Y., Zhang, G., Shen, H., and Xu, Y. J.: Nonlinear Response of Streamflow to Climate

966   Change in High-Latitude Regions: A Case Study in Headwaters of Nenjiang River Basin in

967   China's Far Northeast, Water, 10, 294, https://doi.org/10.3390/w10030294, 2018.

968   Yuan, X., Zhang, M., Wang, L., and Zhou, T.: Understanding and seasonal forecasting of

969   hydrological drought in the Anthropocene, Hydrol. Earth Syst. Sci., 21, 5477–5492,

970   https://doi.org/10.5194/hess-21-5477-2017 , 2017.

971   Zhang, W., Mei, X., Geng, X., Turner, A. G., and Jin, F.-F.: A Nonstationary ENSO–NAO

972   Relationship Due to AMO Modulation, J. Clim., 32, 33–43, https://doi.org/10.1175/JCLI-D-18-

973   0365.1, 2019.

974   Zhang, X., Jin, L., Chen, C., Guan, D., and Li, M.: Interannual and interdecadal variations in

975   the North Atlantic Oscillation spatial shift, Chin. Sci. Bull., 56, 2621–2627,

976   https://doi.org/10.1007/s11434-011-4607-8, 2011.

977